Journal of Power Sources 196 (2011) 7251–7256

Contents lists available at ScienceDirect

Journal of Power Sources

journal homepage: www.elsevier.com/locate/jpowsour

Effect of Mn–Co spinel coating for Fe–Cr ferritic alloys ZMG232L and 232J3 for solid oxide fuel cell interconnects on oxidation behavior and Cr-evaporation

Toshihiro Uehara[a,*], Nobutaka Yasuda[a], Masayuki Okamoto[b], Yoshitaka Baba[c]

[a] Hitachi Metals, Ltd., Metallurgical Research Laboratory, 2107-2 Yasugi-cho, Yasugi-shi, Shimane 692-8601, Japan
[b] Hitachi Metals, Ltd., Kuwana Works, 210 Obuke, Asahi-cho, Mie-gun, Mie 510-8102, Japan
[c] Tokyo Gas Co., Ltd., 3-13-1 Minami-Senju, Arakawa-ku, Tokyo 116-0003, Japan

ARTICLE INFO

Article history:
Received 23 June 2010
Received in revised form
17 November 2010
Accepted 17 November 2010
Available online 24 November 2010

Keywords:
SOFC
Interconnect
Alloy
Oxidation
Coating
Evaporation

ABSTRACT

Metallic materials, especially Fe–Cr ferritic alloys, are promising as interconnect materials of solid oxide fuel cells (SOFCs) operated at around medium temperatures. ZMG232L is one of the developed Fe–Cr ferritic alloys for SOFC metallic interconnects.

These metallic materials are usually machined or pressed into various shapes of interconnect parts, and thickness of these parts is often thin. However, the oxidation rate of thin sheet was much higher than that of thick one because Cr content decreased under oxide layer of edge part of thin sheet. Such accelerated oxidation behavior could be improved by reducing Mn, increasing Cr, and adding W in ZMG232L.

It is also very important to reduce Cr-evaporation from the oxidized surface of ferritic alloys in cathode side. The aim of this study is to reduce the Cr-evaporation from oxidized alloy surface in air by coating with Mn–Co spinel oxide. In this study, oxidation behavior and Cr-evaporation of ZMG232L and improved Fe–Cr alloy, 232J3, coated with Mn–Co spinel oxide were investigated at elevated temperature in air. $MnCo_2O_4$ spinel coating on the pre-oxidized Fe–Cr ferritic alloy surface improved oxidation resistance and Cr-evaporation.

1. Introduction

In late years, according to the reduction of operating temperature of SOFCs to lower than about 850 °C, Fe–Cr ferritic alloys are thought to be promising as interconnect materials of SOFCs because of their low thermal expansion behavior close to ceramic parts, relatively good oxidation resistance, lower cost than ceramics, good workability, good machinability, and so on. However, conventional Fe–Cr ferritic alloys such as type 430 stainless steel do not have sufficient oxidation resistance at medium operating temperature of SOFCs (around 700–850 °C). ZMG232L is one of the developed Fe–Cr ferritic alloys especially for SOFC metallic interconnects and this alloy is being tested in various types of stacks in power generation conditions. This alloy is a Fe–22mass%Cr ferritic alloy with a small addition of Zr and La and reduction of Si and Al, which has good oxidation resistance and good electrical conductivity at elevated temperature in the range of about 700–1000 °C required for SOFC interconnects [1–3]. Oxidation of thin specimen of ZMG232L at 850 °C in air was accelerated as the thickness became small. This was attributed to the rapid depletion of Cr at the edge part of thin sheet [4,5]. Such accelerated oxidation behavior could be improved by reducing Mn, increasing Cr, and adding W in ZMG232L [6]. In order to improve the durability and lifetime performance of Fe–Cr alloy interconnects in addition to improvement of its oxidation resistance, it is very important to prevent Cr evaporation from the surface of Fe–Cr alloy in air. Therefore, an improved Fe–Cr alloy, 232J3, was developed by changing Mn content to control the thickness of Mn–Cr spinel top layer formed on the alloy surface [7]. Another approach to prevent Cr evaporation is to apply protective oxide coating on the alloy surface. One of the promising protective oxide coatings on Fe–Cr alloys is Mn–Co spinel oxide and this coating is also effective to improve oxidation resistance of Fe–Cr alloy substrate [8,9].

In this study, Mn–Co spinel coating was carried out on ZMG232L and an improved Fe–Cr alloy, 232J3, for SOFC interconnects and its effect on oxidation resistance and Cr evaporation and migration was investigated to improve the long-term durability (*Note*: ZMG is a trademark of Hitachi Metals, Ltd.).

2. Experiments

2.1. Specimen

The chemical compositions of ZMG232L and an improved alloy, 232J3, are shown in Table 1. 232J3 which contains higher Cr, lower Si and Al, and a little lower Mn than ZMG232L, and moreover

* Corresponding author. Tel.: +81 854 22 1979; fax: +81 854 22 6374.
E-mail address: toshihiro_uehara@hitachi-metals.co.jp (T. Uehara).

0378-7753/$ – see front matter © 2010 Elsevier B.V. All rights reserved.
doi:10.1016/j.jpowsour.2010.11.078

Table 1
Chemical compositions of alloys for this study (mass%).

Alloy	C	Si	Mn	Ni	Cr	Al	Zr	La	W	Fe
ZMG232L	0.02	0.08	0.48	0.36	22.0	0.07	0.23	0.07	–	bal.
232J3	0.03	0.01	0.27	0.38	23.8	0.01	0.25	0.09	1.98	bal.

contains W has thinner oxide layer than ZMG232L after exposure at elevated temperature, and consequently has better oxidation resistance even though it is shin sheet. These alloys were melted in vacuum and cast into ingots, and then hot forged and finally annealed. Test pieces were cut from the annealed bar and machined into plates with 3 mm thick and 10 mm square, and then polished. The test pieces before coating were prepared as polished and as pre-oxidized at 900 °C for 8 h in air after polished, which was the condition in which approximately 1 μm thick oxide layer was formed on ZMG232L. $MnCo_2O_4$ spinel oxide was selected for protective coating on ZMG232L and 232J3 because it has close coefficient of thermal expansion to those of Fe–Cr ferritic alloys and good electrical conductivity. Various methods of $MnCo_2O_4$ spinel oxide coating such as screen printing, dipping, plasma spraying and PVD are applied for protective coating. In this study $MnCo_2O_4$ was coated by screen-printing technique because of its easy control of thickness of coated layer and easy application for small test pieces. Screen-printed $MnCo_2O_4$ spinel was not fully densified at low temperature that the alloy can withstand, so the following method was introduced. At first, 5% of $LiNO_3$ as a sintering aid was added into an $MnCo_2O_4$ slurry. After that, it was stirred thoroughly by a ball mill, the slurry was screen-printed on one-sided surface (10 mm × 10 mm area) of the alloy substrate. Further, in order to fully densify the spinel coating the samples were reductional-fired in N_2/H_2 (4%) atmosphere at 800 °C for 20 h and finally fired in air at 850 °C for 10 h.

2.2. Oxidation test

Each test piece was put in a ceramic container, and put into an electric furnace at 850 °C in air. The test temperature of 850 °C was chosen as an accelerated condition [5]. The oxidation weight gain of each test piece was measured after each 500 h oxidation test at 850 °C in air. After the measurement, the specimen was cut, plated with Ni, mounted in the resin, ground and polished, and then the cross-sectional microstructure of coating layer and oxide layer at the interface between alloy and coating layer was observed and analyzed with scanning electron microscopy (SEM) and electron probe microanalyser (EPMA).

2.3. Cr evaporation test

Each test piece was put between ceramic plates, and put into the electric furnace at 850 °C for 30 h in air. The 0.4 mm gap was made between the upper ceramic plate and the surface of the test piece with ceramic spacers, as shown in Fig. 1. After exposure, the amount of Cr deposited on the surface of ceramic plate facing the test piece was analyzed by energy dispersion spectroscopy (EDS). Area of analysis was about 0.3 mm × 0.3 mm square. The analyzed value of deposited Cr concentration on the surface of ceramic plate evaporated from the coated specimen was divided by that from the uncoated ZMG232L specimen. This value shows deposited Cr amount compared with that evaporated from the uncoated ZMG232L.

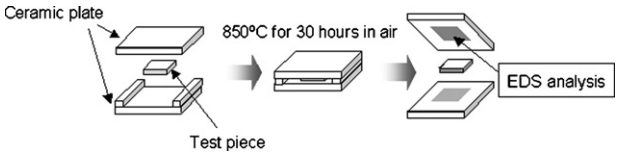

Fig. 1. Method of Cr-evaporation test.

2.4. ASR measurement

ASR property is important to know the effect of metallic interconnects for the power generation performance. Test pieces of 3 mm × 10 mm × 10 mm with and without coating on one side (10 mm × 10 mm area) were used for ASR measurement. Test pieces were covered with Pt-paste for connection with a standard Pt-mesh on both of the 10 mm × 10 mm areas and ASR was measured in air at 750 °C after exposure in air at 850 °C for 1000 h using a four-point method.

3. Results and discussion

3.1. Oxidation behavior

Oxidation weight gain at 850 °C in air as a function of exposure time is shown in Fig. 2. Improved alloy, 232J3, indicated smaller oxidation weight gain than ZMG232L with and without pre-oxidation, as well as with and without $MnCo_2O_4$ spinel coating. Oxidation weight gain of 232J3 without coating was smaller than half of that of ZMG232L without coating. Therefore, it was found that 232J3 showed much better oxidation resistance than ZMG232L. Pre-oxidized specimens of ZMG232L and 232J3 indicated a little

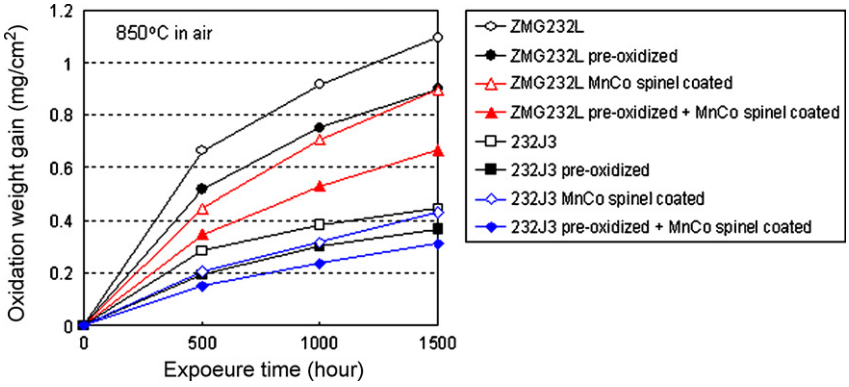

Fig. 2. Oxidation weight gain of ZMG232L and 232J3 with and without coating as a function of exposure time at 850 °C in air.

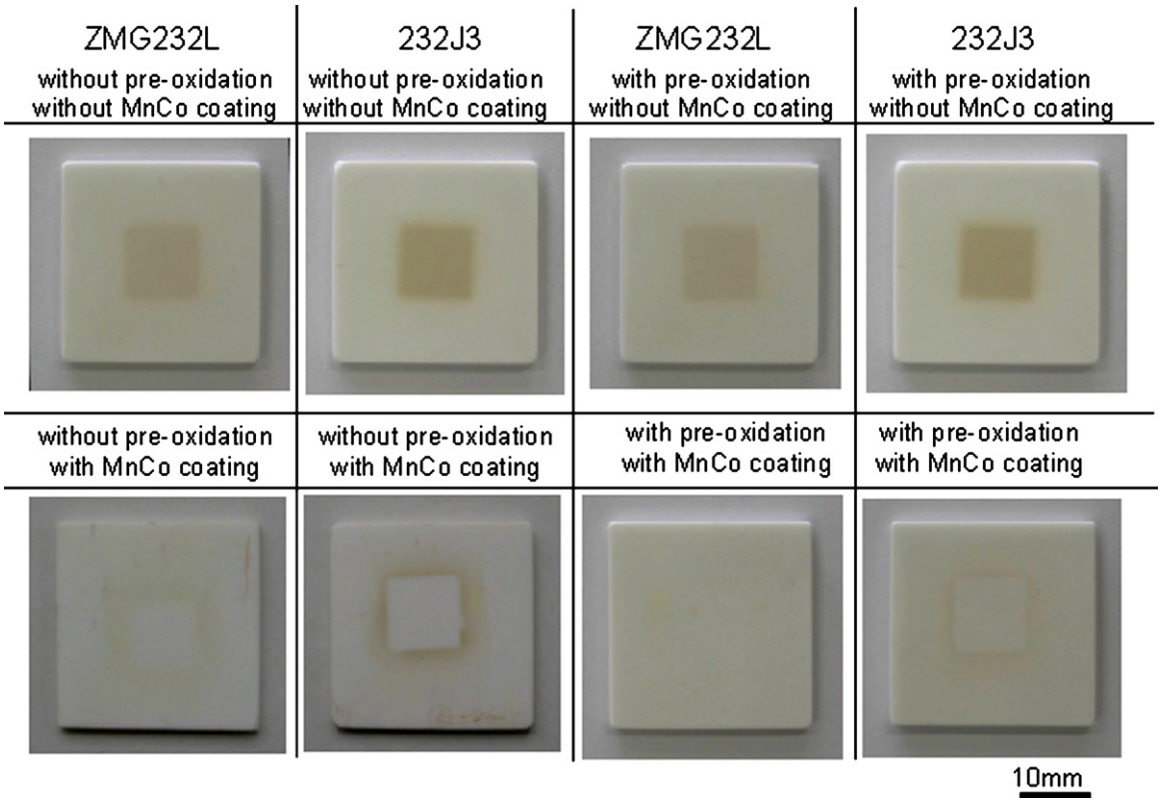

Fig. 3. Appearance of ceramic plates after Cr evaporation test at 850 °C for 30 h in air.

smaller oxidation weight gain than ZMG232L and 232J3 without pre-oxidation. Pre-oxidation is thought to be a little effective to oxidation resistance. This should be attributed to the formation of thin and dense oxide layer on the surface of alloy by pre-oxidation and this retards the growth of oxidation layer during the oxidation test.

$MnCo_2O_4$ spinel coating reduced oxidation weight gain of ZMG232L and 232J3. The reduction of oxidation weight gain of ZMG232L was larger than that of 232J3, although its oxidation weight gain was larger than that of 232J3. The oxidation weight gain of coated specimen was comparable to that of pre-oxidized one. Since $MnCo_2O_4$ spinel oxide layer was coated only on the one-side surface (10 mm × 10 mm) of specimen, $MnCo_2O_4$ spinel coating was more effective than pre-oxidation regarding the oxidation resistance. $MnCo_2O_4$ spinel coating was also effective for pre-oxidized specimen. The oxidation weight gain of specimen with both of pre-oxidation and of $MnCo_2O_4$ spinel coating was the smallest. As for oxidation resistance, the best one was 232J3 with both of pre-oxidation and of $MnCo_2O_4$ spinel coating in this study.

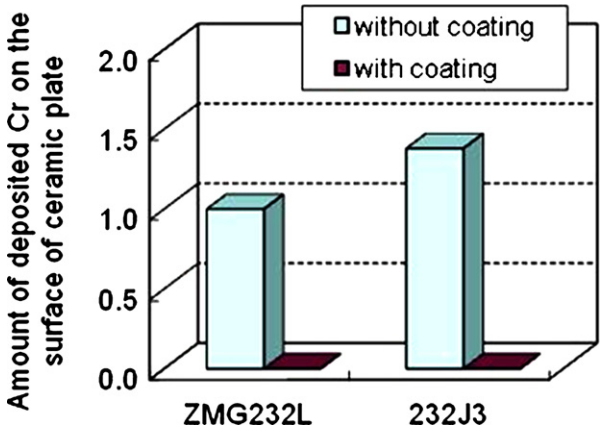

Fig. 4. Amount of deposited Cr on the surface of ceramic plate above test piece with and without coating after exposure at 850 °C for 30 h in air (vertical axis shows the each deposited Cr amount detected with SEM-EDS analysis divided by that evaporated from uncoated ZMG232L, analyzed area: 0.3 mm × 0.3 mm square).

3.2. Cr evaporation and migration behavior

Appearance of ceramic plates where evaporated Cr was deposited after Cr evaporation test at 850 °C for 30 h in air is shown in Fig. 3, and the amount of Cr on the ceramic plates by EDS analysis is shown in Fig. 4. Evaporated Cr was deposited at the brown-coloured area of the ceramic plate from the EDS analysis. Brown-coloured square area for specimens without coating corresponds to the Cr evaporation area from the upper surface (10 mm × 10 mm) of the test piece. On the other hand, white square area surrounded by light brown-coloured frame was observed on ceramic plate for specimen with $MnCo_2O_4$ spinel coating. It was found that $MnCo_2O_4$ spinel coating prevented Cr from evaporating from the coated surfaces of these specimens. Here, it is noted that light brown-coloured frame area shown in Fig. 3 is due to Cr deposition evaporated from the uncoated side areas of the specimen with coating. As shown in Fig. 4, amount of deposited Cr from 232J3 without coating was a little higher than that from ZMG232L without coating. This is thought to be attributed to the thinner oxide layer on the surface of 232J3 than that of ZMG232L. On the other hand, no deposited Cr from both of 232J3 and of ZMG232L was detected in this white square area as shown in Fig. 4. This is because protective $MnCo_2O_4$ coating prevented Cr from evaporating from the alloy surface (For interpretation of the references to colour in this figure legend, the reader is referred to the web version of this article.).

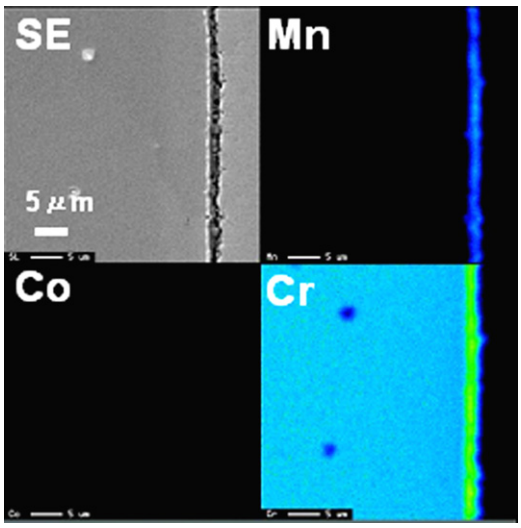

Fig. 5. Cross-sectional EPMA element map of ZMG232L with pre-oxidation.

Cross-sectional EPMA element map of ZMG232L with pre-oxidation is shown in Fig. 5. Top layer of Mn–Cr spinel oxide and the second layer of Cr oxide were formed by pre-oxidation at 900 °C for 8 h in air. This oxide layer formed by pre-oxidation was thin and homogenous. Cross-sectional EPMA element maps of coated surfaces of specimens as coated and after exposure at 850 °C for 500 h in air are shown in Figs. 6 and 7, respectively. As coated, Cr oxide was formed between the alloy surface and $MnCo_2O_4$ spinel layer both of ZMG232L and of 232J3 with and without pre-oxidation, and Cr oxide layer of 232J3 was a little thinner than that of ZMG232L. Furthermore Cr oxide layers with pre-oxidation of ZMG232L and 232J3 were thinner than those without pre-oxidation, as coated. As for the Cr oxide layers as coated, Cr oxide layers of ZMG232L and 232J3 without pre-oxidation were formed during firing of coating layers, although Cr oxide layers of these alloys with pre-oxidation were mainly formed during pre-oxidation. Pre-oxidation is thought to be effective to form thin and homogenous oxide layer between the alloy and coating layer.

After exposure at 850 °C for 500 h, Cr oxide layers of ZMG232L and 232J3 without pre-oxidation slightly grew, and Cr diffused into $MnCo_2O_4$ spinel coating layer and obviously concentrated on the top surface of coating layer. On the other hand, Cr oxide layers and Mn–Cr spinel oxide layers of ZMG232L and 232J3 with pre-oxidation did not grow and Cr did not diffuse into the coating layer very much after exposure. Only small amount of Cr was detected on the top surface of coating layer of 232J3 because Cr oxide layer and Mn–Cr spinel oxide layer of 232J3 was thinner than that of ZMG232L. From this result, it can be seen that pre-oxidation is very effective to prevent Cr from diffusing from alloy side to $MnCo_2O_4$ spinel coating layer. It is thought that Mn–Cr spinel oxide layer is formed on Cr oxide layer by pre-oxidation and can retard Cr migration into coating layer. Therefore, the optimisation of chemical

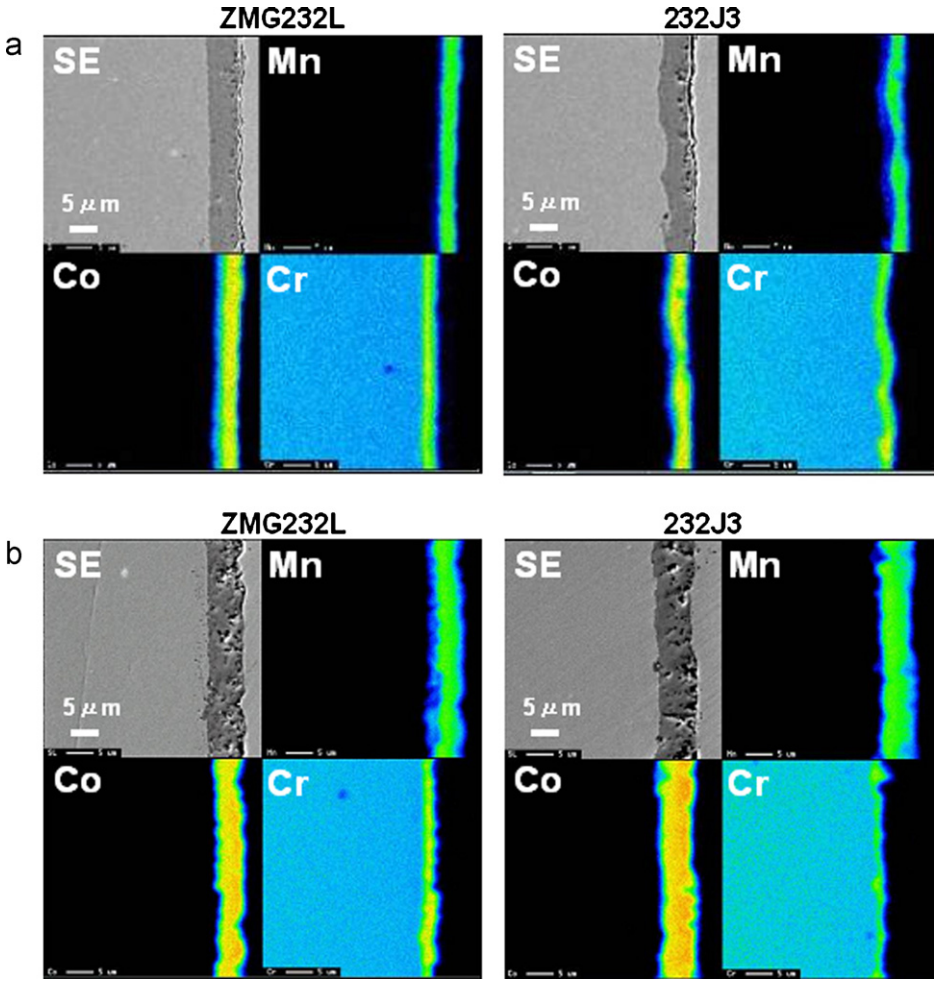

Fig. 6. Cross-sectional EPMA element maps of the surface of specimens with $MnCo_2O_4$ spinel coating as coated. (a) As-coated specimens without pre-oxidation coated with MnCo spinel, (b) as-coated specimens with pre-oxidation coated with MnCo spinel.

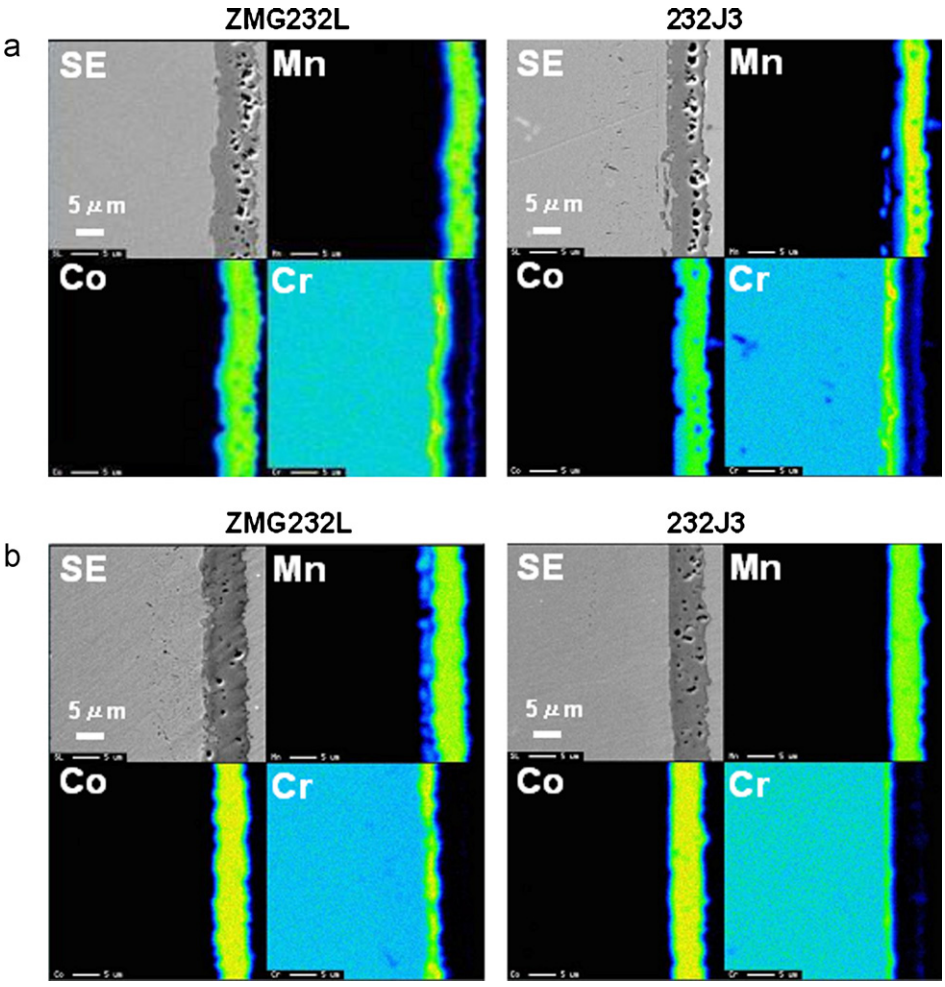

Fig. 7. Cross-sectional EPMA element maps of the surface of specimens with $MnCo_2O_4$ spinel coating after exposure at 850 °C for 500 h in air. (a) Specimens without pre-oxidation coated with MnCo spinel after exposure at 850 °C, (b) specimens with pre-oxidation coated with MnCo spinel after exposure at 850 °C.

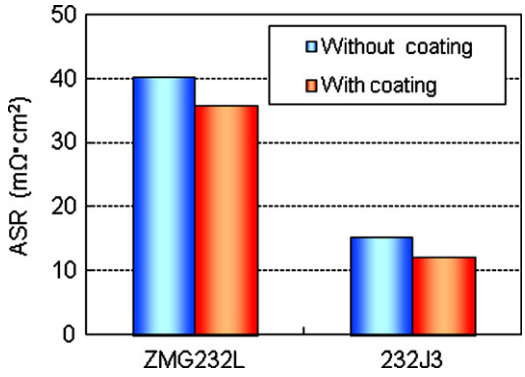

Fig. 8. ASR of both sides measured at 750 °C after exposure at 850 °C for 1000 h in air (coating was carried out on one side of 10 mm × 10 mm area).

compositions of alloy as well as morphology of oxide layers under $MnCo_2O_4$ spinel coating layer is considered to be very important to reduce Cr migration and evaporation.

3.3. ASR property

ASR measured at 750 °C after exposure at 850 °C for 1000 h in air is shown in Fig. 8. ASR values of ZMG232L and 232J3 with $MnCo_2O_4$ spinel coating are almost as same as those without this coating. The thickness of oxide layer of alloy with coating is thinner than that of alloy without coating because the oxidation weight gain of alloy with coating is smaller than that of alloy without coating as shown in Fig. 2. On the other hand, total thickness of coated layer and oxide layer formed along the interface between alloy and coated layer is larger than thickness of only oxide layer formed on the surface of alloy without coating. The electrical conductivity of $MnCo_2O_4$ spinel layer is thought to be lower than chromia layer formed on the alloy surface. Therefore, it seems that total ASR value of alloy with coating is comparable to that without coating.

From comparison of ASR between ZMG232L and 232J3, ASR of 232J3 is much lower than that of ZMG232L, regardless of coating, as shown in Fig. 8. From Fig. 2, the oxidation weight gain of 232J3 with and without coating is much smaller than that of ZMG232L, and from Figs. 6 and 7, the oxide layer formed between 232J3 alloy and coated layer is thinner than that between ZMG232L alloy and coated layer. Therefore, the low ASR value obtained in 232J3 is due to the thinner oxide layer formed on the surface of 232J3 than ZMG232L.

As a result, it is found that $MnCo_2O_4$ spinel coating does not significantly influence the electrical property of alloy.

4. Conclusions

The effect of $MnCo_2O_4$ spinel coating on the properties of ZMG232L and an improved alloy, 232J3, was investigated. Oxidation resistance was improved by $MnCo_2O_4$ spinel coating, and it was further improved by applying pre-oxidation before coating.

Cr-evaporation was significantly reduced by $MnCo_2O_4$ spinel oxide layer, although Cr migration was observed into the coating layer. Pre-oxidation retarded Cr migration into the coating layer. It is thought that combination of alloy design of Fe–Cr ferritic alloy and application of protective coating on the alloy surface is important to satisfy the required properties for metallic interconnects.

Acknowledgement

This study was supported by New Energy and Industrial Technology Research Development Organization (NEDO).

References

[1] A. Toji, T. Uehara, Proceedings of 7th European SOFC Forum, in: J.A. Kilner (Ed.), CD-ROM Version, European Fuel Cell Forum, Switzerland, 2006.
[2] A. Toji, T. Uehara, in: K. Eguchi, S.C. Singhal, H. Yokokawa, J. Mizusaki (Eds.), SOFC-X, ECS Transactions 7 (2) (2007) 2117–2124.
[3] T. Horita, K. Yamaji, N. Sakai, H. Yokokawa, A. Toji, T. Uehara, T. Seo, K. Ogasawara, H. Kameda, Y. Matsuzaki, S. Yamashita, in: K. Eguchi, S.C. Singhal, H. Yokokawa, J. Mizusaki (Eds.), SOFC-X, ECS Transactions 7 (2) (2007) 2363–2370.
[4] T. Uehara, N. Yasuda, T. Ohno, A. Toji, Electrochemistry 77 (2009) 131–133.
[5] T. Uehara, N. Yasuda, M. Okamoto, C. Aoki, T. Ohno, T. Toji, in: S.C. Singhal, H. Yokokawa (Eds.), SOFC-XI, ECS Transactions 25 (2) (2009) 1455–1462.
[6] N. Yasuda, T. Uehara, M. Okamoto, C. Aoki, T. Ohno, T. Toji, in: S.C. Singhal, H. Yokokawa (Eds.), SOFC-XI, ECS Transactions 25 (2) (2009) 1447–1453.
[7] N. Yasuda, T. Uehara, M. Okamoto, K. Yamamura, Proceedings of 9th European SOFC forum, in: T. John, S. Irvine (Eds.), CD-ROM Version, European Fuel Cell Forum, Switzerland, 2010.
[8] Z. Yang, G. Xia, J.W. Stevenson, Electrochemical Solid State Letters 8 (3) (2005) A168–A170.
[9] Y. Baba, K. Ogasawara, H. Kameda, Y. Matsuzaki, S. Yamashita, N. Yasuda, T. Uehara, T. Seo, T. Horita, K. Yamaji, H. Yokokawa, 214th Meeting of the Electrochemical Society (PriME 2008), Abstract 1346.